International Journal of Modern Physics B
Vol. 22, Nos. 18 & 19 (2008) 2823–2832

World Scientific
www.worldscientific.com

SUPERPLASTIC INDENTATION CREEP OF FINE-GRAINED Sn-1% Bi ALLOY

REZA MAHMUDI

School of Metallurgy and Materials Engineering, University of Tehran, Tehran, Iran
mahmudi@u

H. MHJOUBI

School of Metallurgy and Materials Engineering, University of Tehran, Tehran, Iran

P. MEHRARAM

School of Metallurgy and Materials Engineering, University of Tehran, Tehran, Iran

Received 20 June 2008

Creep and superplasticity of the fine-grained Sn-1wt.% Bi alloy, processed by conventional rolling (CNR), cryorolling (CRR) and equal channel angular pressing (ECAP) routes, were investigated by indentation testing at room temperature ($T > 0.6T_m$). Based on the steady-state power law creep relationship, the stress exponents of 4.1, 2.8 and 2.5 were obtained for the CNR, CRR and ECAP routes, respectively. The corresponding strain rate sensitivity (SRS) indices of 0.24, 0.36 and 0.40, corresponding respectively to the grain sizes of 2.8, 2.1 and 1.2 μm, indicate that the materials processed by ECAP and CRR exhibit superplastic deformation behavior for which, grain boundary sliding is the possible creep mechanism.

Keywords: Indentation creep; Superplasticity; ECAP.

1. Introduction

One of the main prerequisites for superplastic deformation is the very small size of the grains, preferably of high angle type. These grains are traditionally obtained by suitable thermo-mechanical treatments in which, fine grains are formed by a combination of cold working and recrystallization. Recent developments in the field of severe plastic deformation have stimulated interests in the achievement of suitable microstructures for superplastic deformation. Processes such as equal channel angular pressing (ECAP), cryorolling (CRR) and asymmetric rolling have all proved to be capable of generating very fine grains with mainly high angle grain boundaries.[1-4] Superplastic deformation behavior of ECAP'd copper,[5] aluminum alloys[6-7] and magnesium alloys[8-9] has been

widely investigated. Deformation at cryogenic temperatures, however, has mainly been carried out to enhance strength properties rather than superplasticity.[10-11]

Among different possible ways of investigating superplastic deformation behavior of materials, indentation methods are of special interest. This is because they can be particularly advantageous when the material is only available as small test-pieces or there are some difficulties with the machining of samples made of very soft materials.[12] In the indentation creep test a constant load is applied on the surface of a sample with a suitable indenter over a period of time. Therefore, plastic yielding and creep take place as the indenter penetrates the material. The variation in penetration depth or the indentation size, expressed as a change in diagonal length, is monitored with dwell time. Thus, the time-dependent flow behavior of materials can be studied by these simple hardness tests. This technique has been used for studying the superplastic creep behavior of different materials. The superplasticity of Sn-37%Pb eutectic[13], Sn-40%Pb-2.5%Sb peritectic[14] and Zn-22%Al eutectoid[15] alloys, investigated by indentation methods, has shown that the parameters which are commonly considered as characteristics of superplasticity can be obtained by these simple tests. One of these parameters is the strain rate sensitivity (SRS) index, *m,* which can be used to asses the superplastic behavior.

The aim of this paper is to investigate the superplastic indentation creep behavior of the fine-grained Sn-1%Bi alloy at room temperature ($T>0.6T_m$), by measuring the stress exponents and SRS indices for the alloys having different grain sizes, obtained by conventional rolling, cryorolling and equal channel angular pressing.

2. Experimental Procedure

2.1. *Materials and processing*

The material used was a tin based alloy containing 1 wt.% Bi. It was prepared from high purity tin and bismuth, melted in an electrical furnace under an inert argon atmosphere, and cast into 130x30x13 mm slabs. To ensure that the slabs had similar initial microstructures, the slabs were homogenized at 425 K for 8h. In order to generate homogeneous fine-grained materials without the initial as-cast dendritic structure, the cast slabs were processed in three different ways. One group of the cast slabs was conventionally rolled down to 2 mm thickness at room temperature *($T>0.5T_m$).* Some other slabs were cryogenically rolled to the same thickness of 2 mm at -50 ^{o}C. In this processing route, the slabs were held in a mixture of dry ice and ethanol for 10 minutes before each rolling pass. The last group of slabs was cut into billets with an initial size of 10 mm×10 mm× 80 mm for processing by ECAP. Pressings were conducted at room temperature using a solid die having an angle between the two channels of 90° and an angle of 20° at the outer arc of curvature at the point of intersection of the two channels. This configuration leads to an imposed strain of 1 on each passage through the die. Samples were sprayed with an MoS_2 lubricant and pressed at a speed of 0.5 mm/s for 4 passes through the die. The samples subjected to repetitive pressings were rotated by 90° in the same sense between each pass in the procedure designated route B_C.

The processed samples were annealed at room temperature for 20 days to stabilize the microstructure before indentation creep testing. The specimens were examined by SEM to observe the grain size and structure of the materials. These specimens were polished to a 0.25 microns diamond finish, followed by polishing on a microcloth without any abrasive. Etching was carried out using a 5% nitric acid and 95% alcohol solution. The microstructure of the material was thus revealed and the grain size was measured by the grain count method.

2.2. *Indentation tests*

The specimens were polished and then tested in a SANTAM universal tensile testing machine, capable of performing constant-load indentation tests. A Vickers diamond pyramid with square base was mounted in a holder which was positioned in the center of the vertical loading bar above the specimen. Indentation creep measurements were made on each sample using 10 N load for dwell times up to 120 min. After application of the load, the indentation depth was measured automatically as a function of time by the machine and the data were acquired by a computer. The depth data were converted to the diagonal length based on the geometry of the indenter. The accuracy of the load measurement was $\pm$ 0.1 N and that of the indentation depth was $\pm$ 0.001 mm.

3. Analysis of Indentation Creep

It is generally accepted that the mechanical behavior of metallic materials at homologous temperatures higher than 0.5 can be fairly expressed by the power-law creep in a wide range of strain rates. Thus, for steady-state creep, the high temperature creep rate $\dot{\varepsilon}$ is described by the power law of the type

$$\dot{\varepsilon} = A\sigma^n \exp(-Q/RT) \tag{1}$$

where σ is the applied stress, A is a material parameter, n denotes the stress exponent, Q is the activation energy, T is the temperature, and R is the universal gas constant.

Juhasz *et al.*[16] studied the creep behavior of a superplastic lead–tin alloy using Vickers tests and obtained the stress exponent (n) in steady-state creep of the following form:

$$n = \left[\frac{\partial \ln \dot{d}}{\partial \ln H_V}\right]_d \tag{2}$$

where H_V is the Vickers hardness number, d is the indentation diagonal length, and $\dot{d}$ is the rate of variation in indentation length. This implies that if $\dot{d}$ is plotted against H_V on a double logarithmic scale, a straight line would be obtained, the slope of which is the stress exponent, n.

Sargent and Ashby[17] carried out hot hardness tests on a wide range of materials and proposed a dimensional analysis for indentation creep. According to their model, the displacement rate of an indenter has been derived as:

$$\frac{du}{dt} = \left[-\frac{\dot{\varepsilon}_0}{C_2}\left(\sqrt{A}\right)\right]\left[\left(\frac{C_1}{\sigma_0}\right)\left(\frac{P}{A}\right)\right]^n \tag{3}$$

where A is the projected area of indentation, C_2 is a constant and $\dot{\varepsilon}_0$ is the rate at a reference stress σ_0, n is the stress exponent and P is the applied load. For a pyramid indenter the penetration is proportional to $\sqrt{A}$, i.e.,

$$u = C_3\sqrt{A}\,. \tag{4}$$

Differentiating Eq. (4) with respect to time and substituting into Eq. (3) gives:

$$\frac{dA}{dt} = C_4\dot{\varepsilon}_0 A\left(\frac{P}{A\sigma_0}\right)^n. \tag{5}$$

where C_3 and C_4 are constants. When P is held constant, Eq. (5) can be rewritten as:

$$\left(\frac{1}{H_V}\right)\left(\frac{dH_V}{dt}\right) = -C_4\dot{\varepsilon}_0\left(\frac{H_V}{\sigma_0}\right)^n \tag{6}$$

From Eq. (6), a plot of ln[(-1/*H*v)(*dH*v/*dt)*] versus $\ln(H_V)$ at a constant temperature has a slope of n. Sargent and Ashby have also derived the following relationship between indentation hardness and dwell time:

$$H_V(t) = \frac{\sigma_0}{\left(nC_4\dot{\varepsilon}_0 t\right)^{\frac{1}{n}}} \tag{7}$$

where $H_V(t)$ is the time dependent hardness. Therefore, from Eq. (7) the slope of a plot of $\ln(H_V)$ against $\ln(t)$ at a constant temperature is –1/n.

4. Results and Discussion

The microstructure of the material processed by different deformation regimes is depicted in Fig. 1. As shown in this figure, grain sizes of 2.8, 2.1 and 1.2 μm were obtained for the materials processed by CNR, CRR and ECAP, respectively.

The indentation creep data are shown in Fig. 2, where the indentation diagonal length is plotted against dwell time. It can be seen that the indentation length increases with the loading time for all three conditions of the material. The shape of the indentation curves is similar to that of an ordinary creep curve. The first stage of the curve records an increase in the concerned variable with time, with a decreasing rate, followed by a steady-state region where indentation sizes increase linearly with time. As the hardness test is actually a compression test, fracture of the specimen does not occur and hence it is obviously not possible to record a third stage of the curve as opposed to what happens in an ordinary creep test.[18]

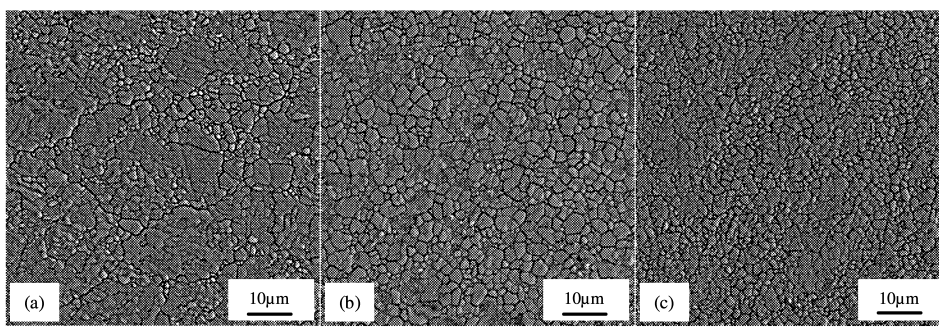

Fig.1. SEM micrographs of the material processed by different routes; a) CNR (d = 2.8 μm); b) CRR (d = 2.1 μm); and c) ECAP (1.2 μm).

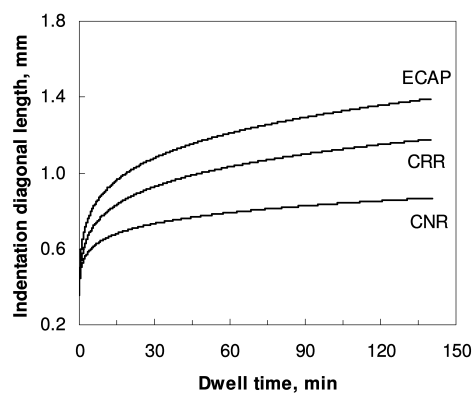

Fig. 2. Indentation creep curves for different conditions of the material.

Fig. 2 also indicates that the materials processed by different deformation regimes exhibit different indentation creep behavior. It can be inferred from this figure that both the level and slope of the curves in the steady state region are higher for the ECAP'd condition having a grain size of 1.2 μm. The CNR condition with d=2.8 μm, however, has the lowest creep rate among all tested conditions. To show this effect more clearly, the rate of variation in indentation diagonal length (do), obtained by differentiation of the curves in Fig. 2, is plotted against dwell time for all materials in Fig. 3. It is observed that there is a steep drop in the creep rates at short dwell times corresponding to the primary creep stage, followed by a lower decreasing rate region which corresponds to the steady-state creep stage of the tested materials. It is further demonstrated that the CNR condition has a lower creep rate than the CRR and ECAP'd materials.

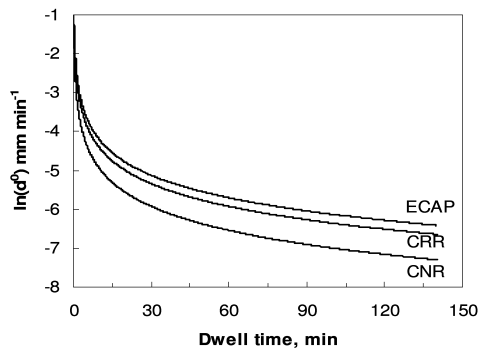

Fig. 3. Rate of variation in indentation length (do) plotted on a semi-log scale against dwell time.

The two aforementioned methods of Juhasz *et al.*[16] and Sargent-Ashby[17] have been applied to the indentation data of the materials to obtain the steady-state creep exponents. Using the Juhasz *et al.* method, Eq. (2), the rate of diagonal variation is plotted against the Vickers hardness number on a double logarithmic scale in Fig. 4.

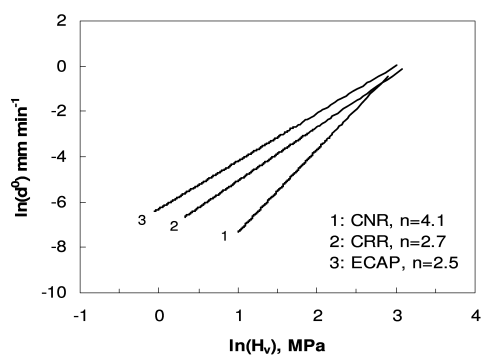

Fig. 4. Plots of ln(d^o) versus ln(Hv) to determine the stress exponent.

A straight line with a slope of n is resulted for each condition. Applying the Sargent-Ashby model, the stress exponent can either be obtained from a plot of $\ln(H_V)$ against $\ln(t)$ with a slope of -1/n or from a plot of ln[(-1/Hv)(dHv/dt)] versus $\ln(H_V)$ with a slope of n. Both of these approaches are illustrated in Figs. 5 and 6 for all conditions.

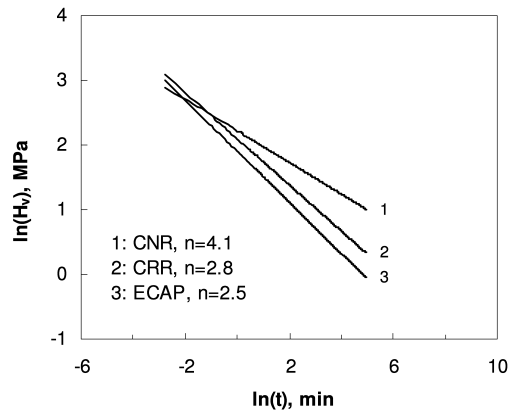

Fig. 5. Hardness-dwell time log-log plots. The slope of these lines will be (-1/n) from which the stress exponent, n, is determined.

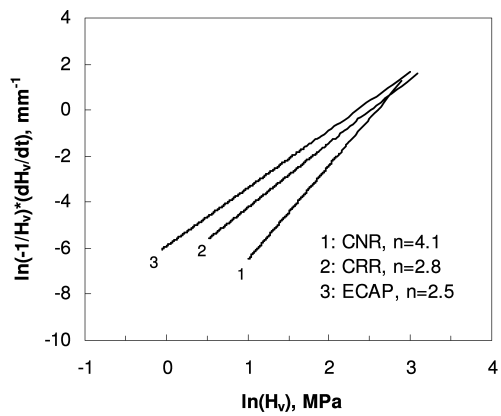

Fig. 6. Plots of ln[(-1/H)(dH/dt)] against ln(H) to determine the stress exponent.

It can be seen that the stress exponent values obtained via each of the abovementioned approaches are in good agreement with each other, indicating the similarity of the derivation methods. The average stress exponents of 4.1, 2.8 and 2.5 obtained respectively for the CNR, CRR and ECAP conditions are given in Table 1 for all material conditions. Also given in this table, are the SRS indices of 0.24, 0.36 and 0.40 found respectively for the CNR, CRR and ECAP conditions.

Table 1. Materials characteristics, stress exponents and SRS indices derived from different methods.

Condition	Grain size (μm)	Stress exponent, *n*	SRS index, *m*
CNR	2.8	4.1	0.24
CRR	2.1	2.8	0.36
ECAP	1.2	2.5	0.40

The observed difference in the indentation behavior, as indicated by different n-values of the tested conditions, can be attributed to their grain sizes and grain types. For the ECAP and CRR conditions, with respective grain sizes of d=1.2 and 2.1 μm, the stress exponents, are 2.5 and 2.8 while for the CNR condition with d=2.8 μm, n is 4.1. This behavior is in agreement with the Gifkins' core-mantle theory suggesting that for a constant width of mantle, an increasingly fine grain size results in a domination of the mantle behavior and thus, the creep exponent begins to decrease.[19] The obtained stress exponents would result in m=1/n values of 0.40, 0.36 and 0.24 for the ECAP, CRR and CNR conditions, respectively.

It is worth noting that although the CNR material possesses a relatively small grain size of 2.8 μm, its SRS index of 0.24 is not as high as those of the CRR and ECAP materials. The microstructure of this condition, shown in Fig. 1a, has a rather non-uniform grain size distribution with colonies of very small grains within larger grains which are believed to be formed as result of static and dynamic recrystallization of the material during room temperature rolling. The presence of some non-equiaxed grains elongated in the rolling direction is evident. Rolling at cryogenic temperatures, however, has significantly suppressed dynamic recrystallization, resulting in more uniform grain structure (Fig. 1b). This is also the case in the ECAP'd material in which, a very uniform fine-grained equiaxed microstructure is developed after 4 passes (Fig. 1c). It seems that both cryogenic deformation and equal channel angular pressing are capable of producing more high angle grain boundaries, while in the conventionally rolled material both high and low angle grain boundaries are present in the microstructure. The relatively high m-values of 0.36 and 0.40 obtained in these conditions are in accord with this argument. It is well accepted that at these relatively high values of SRS index, superplastic deformation mechanisms such as grain boundary sliding become prominent and creep process takes place readily. Similar behavior has been reported by Juhasz *et al.*,[16] who obtained stress exponent values in the range of 2–2.5, corresponding to strain rate sensitivity indices of about 0.45 to 0.5 for a lead-tin eutectic alloy. Other results on the Sn-Pb-Sb peritectic alloy are indicative of $n = 2.6$ and $m = 0.39$.[14] This represents a superplastic deformation behavior in which, grain boundary sliding occurs during indentation creep process.

5. Conclusion

1. It is demonstrated that the indentation creep test provides a convenient method for measuring stress exponents and SRS, and thereby assessing the material's ability to undergo superplastic deformation.

2. The stress exponents calculated from different methods of analysis are in complete agreement with each other. These stress exponents were found to be respectively 4.1, 2.8 and 2.5 for the CNR, CRR and ECAP routes, corresponding to SRS indices of 0.24, 0.36 and 0.40, respectively.

3. Although all of the deformation regimes produced very fine grain sizes in the range 1.2 to 2.8 μm, the uniformity of grain size distribution and the nature of the grain boundaries were quite different. ECAP and cryogenic deformation produced finer structures mainly with high angle grain boundaries, resulting in m-values of 0.40 and 0.36, respectively. These high SRS indices suggest that grain boundary sliding is the main deformation mechanism for the room-temperature creep of these fine-grained alloys.

References

1. T. C. Lowe, R. Z. Valiev, "The Use of Severe Plastic Deformation Techniques in Grain Refinement", JOM, 56, 2004, pp. 64-77.
2. T. S. Wang, J. G. Peng, Y. W. Gao, F. C. Zhang, T. F. Jing, "Microstructure of 1Cr18Ni9Ti stainless steel by cryogenic compression deformation and annealing", Mater. Sci. Eng., A407, 2005, pp. 84-88.
3. Y. B. Lee, D. H. Shin, K. T. Park, W. J. Nam, "Effect of annealing temperature on microstructures and mechanical properties of a 5083 Al alloy deformed at cryogenic temperature", Script. Mater., 51, 2004, pp. 355-359.
4. H. Jin, D. J. Lloyd, "The tensile response of a fine-grained AA5754 alloy produced by asymmetric rolling and annealing", Metall. Mater. Trans., 35A, 2004, pp. 997-1006.
5. K. Neishi, Z. Horita, T. G. Langdon, "Achieving superplasticity in ultrafine-grained copper: Influence of Zn and Zr additions", Mater. Sci. Eng., A352, 2003, pp. 129-135.
6. M. Ferry, N. Burhan, "Microstructural evolution in a fine-grained Al-0.3 wt.% Sc alloy produced by severe plastic deformation", Script. Mater., 56, 2007, pp. 525-528.
7. J. Gubicza, N. Q. Chinh, T. Csanadi, T. G. Langdon, T. Ungar, "Microstructure and strength of severely deformed fcc metals", Mater. Sci. Eng., A462, 2007, pp. 86-90.
8. R. B. Figueiredo, T. G. Langdon, "The development of superplastic ductilities and microstructural homogeneity in a magnesium ZK60 alloy processed by ECAP", Mater. Sci. Eng., A430, 2006, pp. 151-156.
9. Y. Miyahara, Z. Horita, T. G. Langdon, "Exceptional superplasticity in an AZ61 magnesium alloy processed by extrusion and ECAP", Mater. Sci. Eng., A420, 2006, pp. 240-244.
10. Y. Wang, M. Chen, F. Zhou, E. Ma, "High tensile ductility in a nanostructured metal", Nature, 419, 2002, pp. 912-915.
11. T. Shanmugasundaram, B. S. Murty, V. Subramanya Sarma, "Development of ultrafine grained high strength Al–Cu alloy by cryorolling", Script. Mater., 54, 2006, pp. 2013–2017.
12. R. Mahmudi, R. Roumina, B. Raeisinia, "Investigation of stress exponent in the power-law creep of Pb–Sb alloys", Mater. Sci. Eng., A382, 2004, pp. 15-22.
13. G. Cseh, N. Q. Chinh, A. Juhasz, "Indentation curves and viscosity measurements on glasses", J. Mater. Sci. Lett., 17, 1998, pp. 1207-1209.

14. R. Mahmudi, A. Rezaee-Bazzaz, "Superplastic power-law creep of Sn-40Pb-2.5Sb peritectic alloy", J. Mater. Sci., 42, 2007, pp. 4051-4059.
15. R. M. Hooper, C. A. Brooks, "Incubation periods and indentation creep in lead", J. Mater. Sci., 19, 1984, pp. 4057-4060.
16. A. Juhasz, P. Tasnadi, I. Kovacs, "Superplastic indentation creep of lead-tin eutectic", J. Mater. Sci. Lett., 5, 1986, pp. 35-36.
17. P. M. Sargent, M. F. Ashby, "Indentation creep", Mater. Sci. Tech., 8, 1992, pp. 594-601.
18. R. Roumina, B. Raeisinia, R. Mahmudi, "Room temperature indentation creep of cast Pb-Sb alloys", Scripta. Mater., 51, 2004, pp. 497-502.